Biotechnology Reports 25 (2020) e00434

Contents lists available at ScienceDirect

Biotechnology Reports

journal homepage: www.elsevier.com/locate/btre

Optimization of recombinant Zika virus NS1 protein secretion from HEK293 cells

Julieta S. Roldán, Alejandro Cassola, Daniela S. Castillo*

Instituto de Investigaciones Biotecnológicas "Dr. Rodolfo A. Ugalde" (IIBIO), Universidad Nacional de San Martín (UNSAM) - Consejo Nacional de Investigaciones Científicas y Técnicas (CONICET), San Martín, Buenos Aires, Argentina

ARTICLE INFO

Article history:
Received 23 November 2019
Received in revised form 9 January 2020
Accepted 10 February 2020

Keywords:
Zika virus
NS1
Recombinant protein
Mammalian expression system

ABSTRACT

Sensitive, accurate and cost-effective diagnostic tests are urgently needed to detect Zika virus (ZIKV) infection. Nonstructural 1 (NS1) glycoprotein is an excellent diagnostic marker since it is released in a hexameric conformation from infected cells into the patient's bloodstream early in the course of the infection. We established a stable rZNS1-His-expression system in HEK293 cells through lentiviral transduction. A novel optimization approach to enhance rZNS1-His protein secretion in the mammalian expression system was accomplished through 50 nM rapamycin incubation followed by serum-free media incubation for 9 days, reaching protein yields of ~10 mg/l of culture medium. Purified rZNS1-His hexamer was recognized by anti-NS1 antibodies in ZIKV patient's serum, and showed the ability to induce a humoral response in immunized mice. The obtained recombinant protein is a reliable biological tool that can potentially be applied in the development of diagnostic tests to detect ZIKV in infected patients during the acute phase.

1. Introduction

Zika virus (ZIKV), originally discovered in the Ziika forest of Uganda in 1947 [1], is a mosquito-borne flavivirus that has emerged as a global health threat after the 2015 outbreak in Brazil, where devastating congenital defects were documented [2]. Since its isolation until 2007, only sporadic cases were reported in many parts of Africa and Asia, with mild clinical manifestations. The first outbreak occurred in Yap island in 2007 [3], followed by a major outbreak in French Polynesia and the Pacific Islands in 2013 [4]. Thereafter, ZIKV spread throughout the South Pacific and eventually to the Americas in 2015 [2]. The size of the outbreak and links to congenital neurodevelopmental defects prompted the World Health Organization (WHO) to declare ZIKV as a public health emergency of international concern on February 2016 [5].

ZIKV is primarily transmitted to humans from bites of infected *Aedes aegypti* or *Aedes albopictus* mosquitoes [6,7], yet there have also been cases of sexual [8,9] and materno-fetal transmission [10]. Most ZIKV infections are asymptomatic. Among symptomatic cases which develop 6–11 days after infection [11], mild signs such as headache, retro-orbital pain, maculopapular rash, fever, arthralgia, conjunctivitis, edema and vomiting are reported [12]. ZIKV gained attention for its causal link to microcephaly in the children of women infected while pregnant, as well as to Guillain-Barré syndrome (GBS) in adults [13–15]. The former is a neurodevelopmental disorder associated with mental retardation, learning disabilities, behavioral abnormalities, muscle weakness and altered muscle tone; whereas the latter is an autoimmune disease that causes flaccid paralysis [16].

ZIKV is a member of the *Flaviviridae* family, which comprises other major global pathogens such as dengue virus, West Nile virus and yellow fever virus. Flavivirus encapsulate a positive-sense RNA genome that encodes a polyprotein that is co- and post-translationally cleaved into three structural (C, prM and E) and seven nonstructural (NS1, NS2A/2B, NS3, NS4A/4B and NS5) proteins [17]. Nonstructural protein 1 (NS1) is a highly conserved glycoprotein among flaviviruses, which shows a molecular weight of 46−55 kDa depending on its glycosylation status. NS1 exists in multiple oligomeric forms: it is present in infected cells as a dimer and it is secreted as a hexameric soluble lipoparticle [18–22]. Intracellular NS1 has been associated with early steps of viral replication, whereas secreted NS1 has been involved with immune evasion [19,23–25]. The extracellular NS1 hexamer is highly immunogenic during flavivirus infection: high levels of this protein circulate in the bloodstream of infected patients during the acute phase up to the ninth day after the onset of the symptoms, and anti-NS1 IgM or IgG antibodies can be detected within 4–7 or 8 days after the initial

* Corresponding author.
E-mail address: dcastillo@iibintech.com.ar (D.S. Castillo).

https://doi.org/10.1016/j.btre.2020.e00434

exposure, respectively [26–28]. These properties turn NS1 glycoprotein into a good diagnostic marker, allowing flavivirus early detection in infected patients [29].

As with many other mosquito-borne flavivirus diseases, ZIKV epidemics usually occur in low resource populations, where *Aedes* mosquitoes thrive under precarious infrastructure. Given that most of these regions do not have access to expensive equipment for traditional diagnostic methods such as polymerase chain reaction (PCR), as well as stable power to operate the system, a rapid, accurate, sensitive and accessible diagnostic technique is urgently needed for the early detection of ZIKV infected patients [29]. Considering the virus limited detection window period up to 10 days after virus infection [30], and the current lack of vaccine and effective treatments available, early diagnosis can save valuable time for patients that are being treated symptomatically and is critical in preventing ZIKV propagation and in the control of future outbreaks. In this context, development of diagnostic methods based on the detection of NS1 in the blood of infected individuals combined with the detection of IgM and IgG antibodies in a dual test is preferred for an accurate diagnosis [29].

Obtaining a functional ZIKV hexameric NS1 protein for diagnosis is not trivial. Post-translational modifications play a critical role in preserving biological functions of proteins. In the case of NS1, the hydrophilic monomer that is released from the viral polyprotein to the endoplasmic reticulum (ER) lumen contains 12 cysteines that form 6 discrete disulfide bonds, which contribute to its stabilization and correct folding [31,32]. In line with this, mutagenesis reports have shown that the last 3 cysteines are crucial for NS1 maturation, oligomerization and secretion [33]. Following cleavage in the ER, the NS1 monomer is glycosylated by the addition of high-mannose carbohydrate moieties [20,34]. Next, it rapidly forms dimeric species, leading to the acquisition of a partially hydrophobic nature and thus associating with the ER membrane [35]. NS1 traffics from the ER through the Golgi, where dimeric subunits associate to form soluble hexamers and exposed carbohydrates are trimmed and processed to more complex sugars [36,37]. Considering that bacterial expression systems produce recombinant proteins that are usually not soluble and lose their structural and immunological features of the native viral protein, recombinant protein production by mammalian cells is preferred since it allows proper protein folding, post-translational modifications and protein assembly [38]. With this strategy in mind and considering that recombinant expression studies have reported that NS1 multimeric species form spontaneously in the absence of other viral proteins [39,40], the aim of this study consisted of establishing a stable and optimized recombinant ZIKV NS1 (rZNS1) expression system from HEK293 cells in order to purify high yields of the hexameric protein, which could potentially be used in the development of diagnostic tests to detect ZIKV infection. Stable rZNS1-hexa-histidine (His)-expressing HEK293 cells were generated through transduction with a lentiviral vector. Enrichment of positive rZNS1-His-expressing cells was carried out by limiting dilution cloning, obtaining 1E4-C9 clone, which presented the highest intracellular and secreted rZNS1-His protein levels. Optimization of rZNS1-His protein secretion in 1E4-C9 HEK293 cells was achieved with 50 nM rapamycin treatment followed by serum-free media incubation for 9 days, obtaining a 29-fold protein production increase. Purified rZNS1-His hexamer was recognized by anti-NS1 antibodies in ZIKV patient's serum and showed the ability to induce a humoral response in immunized mice. The obtained recombinant protein may be of significant value for the development of improved diagnostic methods for the detection of ZIKV in infected patients during the acute phase.

2. Materials and methods

2.1. Cell culture

HEK293 human embryonic kidney cells were grown in Dulbecco's Modified Eagle Medium (DMEM, Life Technologies) supplemented with 10 % fetal bovine serum (FBS, Natocor), 50 μg/ml gentamicin sulfate (Sigma-Aldrich), 2 mM GlutaMAX (Gibco) and 1 mM sodium pyruvate at 37 °C in a 5 % CO_2 humidified atmosphere. When indicated, cells were washed in Phosphate Buffered Saline (PBS) prior to incubation for the indicated times in serum-free DMEM at 37 °C in 5 % CO_2 supplemented as indicated above.

For hypotonic treatment, cells were incubated in hypotonic medium (PBS 0.45 % glucose, 1 % FBS, 50 mM or 100 mM NaCl) for 1 h. Rapamycin treatment (50 nM or 100 nM, Sigma) was carried out in serum-free DMEM for 2 h. Incubation with Earle's balanced salt solution (EBSS, GIBCO) was performed for 2 h. Following a washing step in PBS, the hypotonic medium, rapamycin supplemented media or EBSS buffer were replaced with serum-free DMEM and cells were incubated for the indicated times. For DMSO treatment, cells were washed in PBS and incubated in 0.25 % or 0.50 % DMSO in serum-free DMEM for the times indicated.

2.2. Lentivirus transduction and cloning

First, lentivirus transfer vector coding for rZNS1 fused to 6xHis was constructed by subcloning the rZNS1-His fragment from the pcDNA3.1 (+) vector (Thermo Fisher plasmid V79020) into the NheI/EcoRI sites of the pLB vector (Addgene plasmid 11619) (Supplementary Fig. 1).

To produce lentivirus, the transfer vector pLB coding for rZNS1-His was cotransfected with the packaging vector pSPAX2 (Addgene plasmid 12260) and the vesicular stomatitis virus (VSV) glycoprotein vector pMD2.G (Addgene plasmid 12259) into HEK293E cells using polyethylenimine (PEI, Polysciences) according to the manufacturer's instructions. Supernatant with lentivirus was collected 2 days after transfection, and low-speed concentration was performed by overnight centrifugation of the viral supernatant at 3000 g and 4 °C. Concentrated viral supernatants were supplemented with 20 mM 4-(2-hydroxyethyl)-1-piperazineethanesulfonic acid (HEPES) pH 7.4 and 12 mg/ml Polybrene (Sigma). For HEK293 transduction, cells were infected with lentivirus by centrifugation at 2500 rpm for 30 min at room temperature (RT). After 4 h of incubation at 37 °C in 5 % CO_2, inoculum was replaced with complete fresh medium. rZNS1-His expression was evaluated by flow cytometry (as described in *2.5. Flow cytometry*). Enrichment of HEK293 cells expressing rZNS1-His was performed cloning twice by limited dilution, obtaining 1E4-C9 and 1E4-D11 clones with ∼90 % rZNS1-His-expressing cells.

2.3. Dot blot

Equal amounts of cell supernatant, 10X supernatant, permeate, ZIKV stock, mock or rZNS1-His (250 ng) were spotted onto a Polyvinylidene Difluoride (PVDF) membrane (Hybond-P, GE Healthcare) with a Bio-Dot microfiltration device (Bio-Rad). Immunoblotting was performed as described in *2.6. Western blotting* using 1:1000 ZNS1 mouse polyclonal sera or 1:200 human sera.

2.4. Immunofluorescence

Cells were fixed with 4 % paraformaldehyde for 10 min at RT, permeabilized with 0.2 % Triton X-100 and incubated with 2 % bovine serum albumin (BSA) in PBS for 1 h at 37 °C. Immunostaining was performed using 1:500 ZNS1 mouse polyclonal sera,

1:2000 Alexa Fluor 488 goat anti-mouse IgG secondary antibody (Invitrogen) and 1.5 μg/μl 4′,6-diamidino-2-phenylindole (DAPI) to visualize nuclei. At least three fields of each stain were randomly selected for analysis. Image acquisition was performed with a Nikon Eclipse E600 microscope at a magnification of 1000 ×. Images were processed with the NIH ImageJ software.

2.5. Flow cytometry

Cells were fixed with 1 % paraformaldehyde for 20 min at 4 °C, permeabilized with cold 90 % methanol in PBS for 30 min at 4 °C, blocked in 2 % BSA in PBS for 1 h at RT and washed in PBS prior to immunostaining with 4 μg/ml ZNS1 monoclonal antibody (mAbia labs, Argentina) O.N. at 4 °C. Following a washing step in PBS, cells were incubated for 1 h at RT with Alexa Fluor 488 goat anti-mouse IgG secondary antibody (Invitrogen) at a 1:100 dilution. Samples were measured with a CyFlow Space cytometer (Partec). Data analysis was performed with WinMDI 2.9 software.

2.6. Western blotting

Cell lysates, cell supernatants, purification fractions, rZNS1-His and gel filtration fractions were resolved on 7 % or 10 % sodium dodecyl sulphate-polyacrylamide gel electrophoresis (SDS-PAGE). After transfer to a nitrocellulose membrane (Hybond-ECL, GE Healthcare), analysis by immunoblotting was performed using 0.2 μg/ml ZNS1 monoclonal antibody (mAbia labs, Argentina), 1:1000 glyceraldehyde 3-phosphate dehydrogenase (GAPDH, Sigma-Aldrich) or 0.1 μg/ml anti-His tag monoclonal antibody (mAbia labs, Argentina). Bound mAbs were recognized with a horseradish peroxidase (HRP) goat anti-mouse IgG secondary antibody (Sigma-Aldrich) at a 1:2000 dilution, Alexa Fluor 680 goat anti-mouse IgG secondary antibody (Invitrogen) at a 1:20000 dilution, or with HRP rabbit anti-human IgG secondary antibody (Dako) at a 1:10000 dilution. The signal was visualized with enhanced chemiluminiscence reagent (GE Healthcare) and CL-XPosure Films (Thermo Scientific), or with an Odyssey Infrared Imager (Li-Cor). Densitometric analysis was performed using the NIH ImageJ software.

2.7. MTT assay

HEK293 rZNS1-His 1E4-C9 cells pretreated or not with rapamycin (as described in *2.1. Cell culture*) were incubated in serum-free media for the indicated times. Cell activity was assessed by 3-[4,5-dimethylthiazol-2-yl]-2,5-diphenyltetrazolium bromide (MTT, Sigma-Aldrich) assay as described previously [41].

2.8. Cell supernatant concentration

Cell supernatants were concentrated ∼10 times by ultrafiltration using a Stirred Ultrafiltration Cell device (Millipore) with a 100 kDa MWCO disc membrane (Millipore).

2.9. Purification

To purify secreted rZNS1-His, supernatant of HEK293 rZNS1-His 1E4-C9 cells treated with 50 nM rapamycin and incubated 9 days in serum-free media were clarified by centrifugation for 5 min at 1500 rpm and subjected to concentration by ultrafiltration as described above. The 10-fold concentrated supernatant was dialyzed in 100 mM NaCl - PBS and loaded on a nickel affinity column (Pharmacia Biotech) O.N. at 4 °C. The column was washed with 50 mM Tris−HCl pH 7.6, 100 mM NaCl, 20 mM imidazole, and rZNS1-His was eluted with 50 mM Tris−HCl pH 7.6, 500 mM NaCl, and 200 mM imidazole. The purification process was confirmed by SDS-PAGE and rZNS1-His fractions were dialyzed against PBS.

2.10. Gel filtration analysis

For gel filtration analysis, rZNS1-His was dialized in 0.01 M phosphate buffer, 0.14 M NaCl, pH 7.4 and used as input for a Superdex 200 Increase 100/300 G L column (GE Healthcare), using the same buffer. Markers used for molecular weight determination were Apoferritin (443 kDa), β-amylase (200 kDa) and Bovine Serum Albumin (66 kDa), all from Sigma. Eluted fractions were resolved by 10 % SDS-PAGE and analyzed by immunoblot (see *2.6. Western blotting*).

2.11. Cross-linking assay

Dialized rZNS1-His (20 μg) was cross-linked with different concentrations of glutaraldehyde (Sigma) for 15 min at 37 °C. Subsequently, the protein samples were mixed with Laemmli buffer, boiled for 5 min, resolved on 7 % SDS-PAGE and analyzed by immunoblot (as described in *2.6. Western blotting*).

2.12. Indirect enzyme-linked immunosorbent assay

Microtiter plates (Nunc Maxisorp 96-well ELISA plates) were coated with 100 μl of rZNS1-His (400 ng/well) in coating buffer (0.1 M Na_2HPO_4 buffer pH 9.5) for 18 h at 4 °C. Following incubation in blocking buffer (5 % skimmed milk in TBS) for 1 h at 37 °C, the plates were further incubated with human sera at a 1:100 dilution, or with mouse polyclonal sera at the indicated dilutions, for 1 h at RT in blocking buffer. Following four washing steps in TBS Tween-20 0.05 %, plates were further incubated in HRP rabbit anti-human IgG secondary antibody (Dako) at a 1:4000 dilution, or with HRP goat anti-mouse IgG Fcγ fragment specific secondary antibody (Jackson Immunoresearch) at a 1:2000 dilution, for 1 h at RT in blocking buffer. Finally, plates were washed four times in TBS Tween-20 0.05 % and after incubation with the substrate [0.3 % H_2O_2, 0.1 % 3,3′,5,5′-tetramethylbenzidine (TMB) in 0.1 M citric acid pH 5] for 15–20 min at RT, the reaction was stopped with 0.2 M H_2SO_4. The absorbance at 450 nm was measured with a FilterMax F5 Multi-Mode microplate reader (Molecular Devices).

2.13. Stock virus growth

ZIKV inactivated stocks were a kind gift from Federico Giovannoni (IQUIBICEN-UBA, CONICET). Briefly, *Aedes albopictus* C6/36 cells were grown in 1.5 % FBS Minimum Essential Media (MEM) and infected with ZIKV PRVABC59 Puerto Rico strain. Supernatants were collected at different time-points to harvest virus. Virus was inactivated by UV radiation as described previously [42].

2.14. Immunizations

Mice were obtained from our own breeding facility and were housed under specific pathogen free (SPF) conditions. 6- to 7-week-old male BALB/c mice were immunized intraperitoneally with 20 μg of rZNS1-His emulsified in complete Freund's adjuvant. Booster injections of 10 μg of rZNS1-His in incomplete Freund's adjuvant were applied 23 and 44 days after the first immunization. The humoral response of a test bleed performed 7 days after the final immunization was assessed by indirect-enzyme-linked immunosorbent assay (iELISA) (see *2.12. Indirect-enzyme-linked immunosorbent assay*). Mice were monitored daily on weekdays. There were no deaths associated to immunizations or care.

2.15. Statistical analysis

Data analysis was performed with GraphPad Prism 5.0 (GraphPad Software, La Jolla, CA, USA). Statistical differences were

assessed by student's *t*-test or analysis of variance (ANOVA) with Bonferroni post hoc analysis for multiple comparisons or with Dunnett post hoc analysis for multiple comparisons to one control group. P-values <0.05 were considered significant.

2.16. Ethical statement

The protocol of animal immunization followed in this study was approved by the Committee on the Ethics of Animal Experiments of the Universidad Nacional de San Martín, according to the recommendations of the Guide for the Care and Use of Laboratory Animals of the National Institutes of Health.

All the sera analyzed in this study came from a previously characterized serum collection provided by the Hospital de Niños "Ricardo Gutierrez". ZIKV-positive sera belong to individuals with positive diagnosis of ZIKV infection. The serum samples had been codified upon collection in order to ensure anonymity of the patients.

3. Results

3.1. Development and characterization of stable HEK293 cell lines expressing rZNS1-His

In order to obtain stable rZNS1-His-expressing HEK293 cells, we first developed the pLB-ZNS1 vector by cloning the rZNS1-His mammalian codon-optimized fragment encoding a chimeric protein composed of a Kozak sequence, followed by the signal peptide of the G protein of VSV, the sequence of MR 766 ZIKV isolate comprising amino acids 791–1142 that correspond to the NS1 polyprotein, and the C-terminal 6xHis tag into the lentiviral transfer vector pLB (Supplementary Fig. 1). Lentivirus were generated by cotransfecting the resulting pLB-NS1 vector with the packaging vector pSPAX2 and the VSV glycoprotein vector pMD2.G into HEK293E cells. HEK293 transduction was carried out by infecting HEK293 cells with the produced lentivirus. rZNS1-His expression was evaluated by immunostaining (Fig. 1A) and flow cytometry (Fig. 1B) in the parental transduced cell line, which showed the stable expression of rZNS1-His protein in 55.2 % of the cell population (Fig. 1B). With the aim to achieve a higher percentage of positive rZNS1-His-expressing cells, clonal cell lines were generated from the parental cells by limiting dilution. 1E4 clone was obtained from the first round of cloning (Fig. 1A), exhibiting 74.9 % of rZNS1-His positive cells (Fig. 1B). Following a second round of cloning, two positive clones were selected after screening (Supplementary Fig. 2): 1E4-C9 and 1E4-D11 (Fig. 1A). These showed 89.6 % and 88.8 % of positive rZNS1-expressing cells, respectively (Fig. 1B). Next, to further characterize the rZNS1-His expression pattern in the clonal cell lines, we performed Western blot assays to determine the intracellular and secreted rZNS1-His protein levels. The results revealed that 1E4-C9 cells presented the highest intracellular (Fig. 1C) and extracellular secreted (Fig. 1D) expression of rZNS1-His protein. Hence, despite the similar percentages of positive rZNS1-expressing cells between 1E4-C9 and 1E4-D11 clonal cell lines observed by flow cytometry, we continued working with 1E4-C9 cells for their significantly higher intracellular and secreted rZNS1-His protein levels.

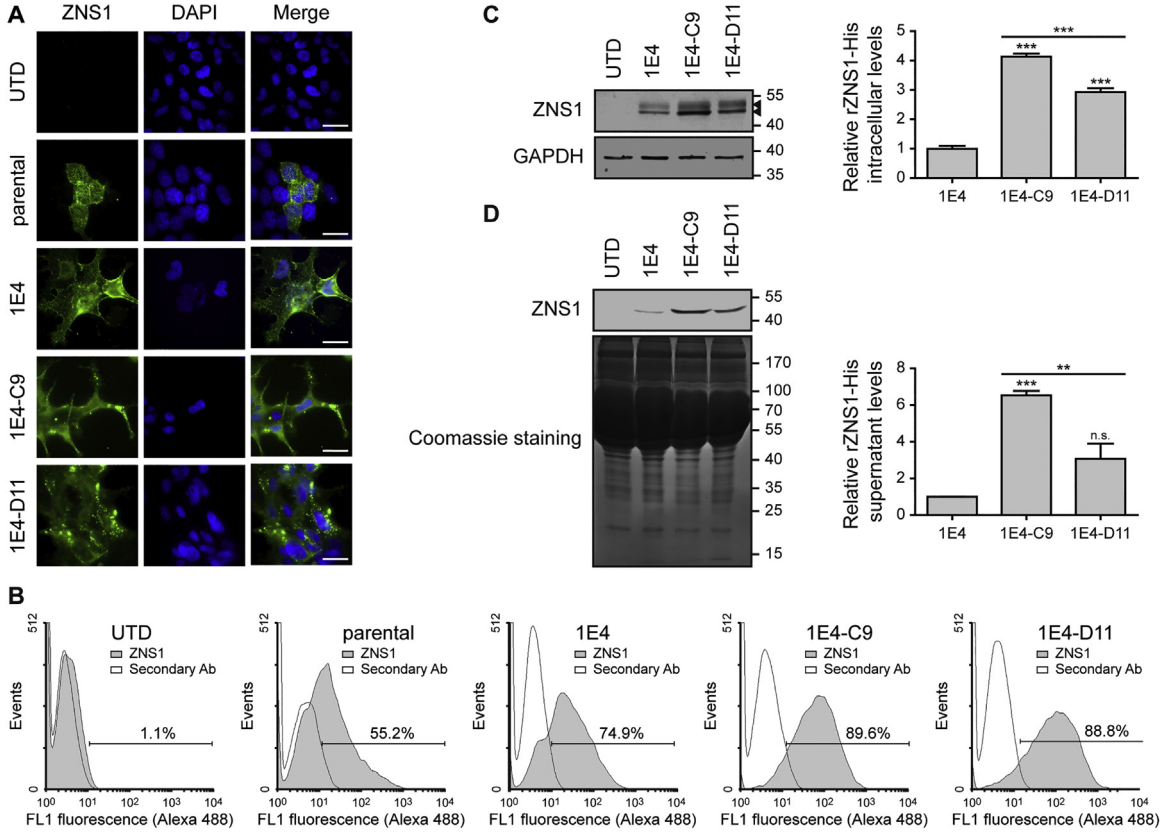

Fig. 1. Development of stable rZNS1-His-expressing HEK293 cells. **(A)** Immunostaining of untransduced (UTD) HEK293 cells, parental, 1E4, 1E4-C9 and 1E4-D11 rZNS1-His HEK293 cells with ZNS1 mouse polyclonal sera. Scale bar, 25 μm. **(B)** Determination of the percentage of positive rZNS1-His-expressing cells assessed by flow cytometry in UTD, parental, 1E4, 1E4-C9 and 1E4-D11 rZNS1-His HEK293 cells. Only secondary Ab was used as control. **(C-D)** Western blot analysis of cell extracts **(C)** and supernatants **(D)** of UTD, 1E4, 1E4-C9 and 1E4-D11 rZNS1-His HEK293 cells with anti-ZNS1 monoclonal antibody. GAPDH **(C)** and Coomassie brilliant blue staining **(D)** were used as loading controls. The position of the molecular mass standards is indicated on the right. Arrowheads in **(C)** indicate rZNS1-His monomer glycosylation pattern. Data represent the mean ± SEM of at least three independent experiments. P-values were calculated by one-way ANOVA, Bonferroni's: $^{**}P < 0.01$, $^{***}P < 0.001$, n.s. not significant.

3.2. Rapamycin treatment and serum depletion increase rZNS1-His secretion in 1E4-C9 HEK293 cells

Given that we sought to purify rZNS1-His in its hexameric conformation, which is the conformation of soluble NS1 secreted into the bloodstream of ZIKV patients during the acute phase of the disease [29], we studied if rZNS1-His protein secretion could be enhanced in 1E4-C9 cells. Previous studies have shown that an increase in protein production in mammalian cells can be achieved by optimizing the culture medium or by the addition of small molecule enhancers (SME) to the media [43]. First, we assessed whether modifications in the culture medium could have an effect on rZNS1-His secretion in 1E4-C9 cells. Considering that several reports have described that serum starvation induces protein expression in human lung A549 epithelial cells [44,45], we tested if serum depletion was capable of enhancing the recombinant protein secretion in our stable HEK293 rZNS1-His-expressing cells. To this purpose, 1E4-C9 cells were incubated in 10 % FBS or serum-free culture medium without media replacement for 5 or 9 days. Under serum depletion conditions, we observed an upregulation of rZNS1-His protein levels in the supernatant of 1E4-C9 cells following 5 and 9 days of incubation by immunoblot assays (Fig. 2A). To further obtain quantitative data of the enhancement effect of serum depletion on 1E4-C9 cells rZNS1-His secretion, we carried out a Western blot assay of supernatants collected at different days after serum-free media addition (Fig. 2B). The results showed that significantly higher rZNS1-His accumulation in the culture media started at day 5, with a maximum at day 9 (Fig. 2C). The time-course analysis of rZNS1-His secretion was performed until day 9 because cell viability was reduced to 38 % at that time point, as assessed by MTT reduction assay (Fig. 2D). The reduced cell viability was expected since serum starvation is considered an 'environmental stress' that is responsible for inducing cell death [46,47]. Next, we studied whether addition of SME could further induce rZNS1-His secretion to the supernatant in serum-starved 1E4-C9 cells. To assess this, we tested the effect of two reported SME that enhance protein production in cultured mammalian cells: rapamycin and dimethylsulfoxide (DMSO) [48–50]. In addition, we analyzed if chromatin relaxation through hypotonic medium treatment a well-documented chromatin-modifying agent [51–53], might render the chromatin structure more accessible to the transcriptional machinery, resulting in increased transcriptional activity and rZNS1-His protein production in 1E4-C9 cells. We performed Western blot assays to determine rZNS1-His protein levels in the supernatant of 1E4-C9 cells harvested 5 or 9 days after rapamycin, DMSO or hypotonic shock treatment followed by incubation in serum-free culture medium. The results revealed a significant 2.4-fold and 2.5-fold increase in rZNS1-His protein secretion in response to the exposure to 50 nM and 100 nM rapamycin at day 9, respectively (Fig. 2E). Addition of DMSO or hypotonic medium treatment did not enhance rZNS1-His production in serum starved 1E4-C9 cells. In previous work, Balcarcel and

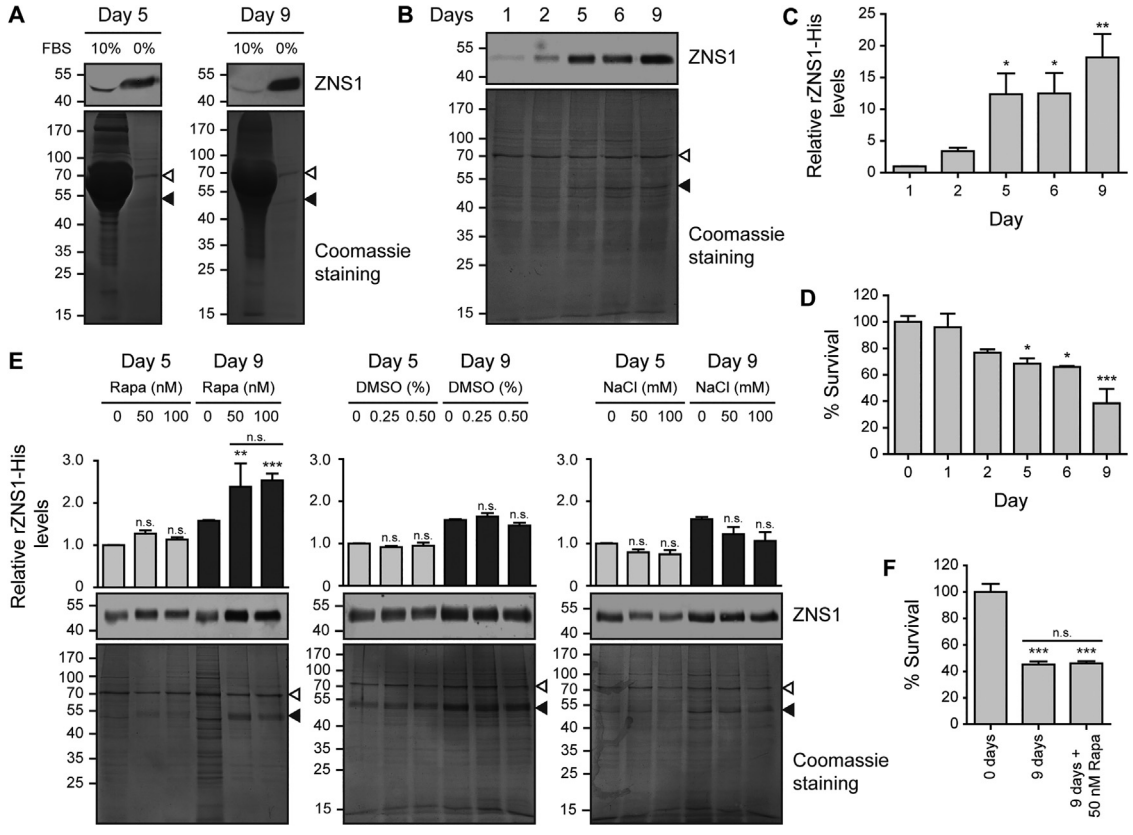

Fig. 2. Optimal conditions for rZNS1-His increased secretion from 1E4-C9 HEK293 cells. **(A-C)** Western blot analysis with anti-ZNS1 monoclonal antibody of supernatants from 1E4-C9 cells incubated in the presence or absence of fetal bovine serum (FBS) **(A)** or in serum-free media for the indicated days **(B-C)**. **(D)** Cell survival assessed by MTT reduction assay in 1E4-C9 cells incubated in serum-free media for the indicated days. **(E)** Immunoblot analysis with anti-ZNS1 monoclonal antibody of supernatants from 1E4-C9 cells subjected to treatment with 50 nM or 100 nM rapamycin (Rapa), 0.25 % or 0.50 % DMSO, or hypotonic medium (50 mM or 100 mM NaCl), followed by incubation in serum-free media for 5 or 9 days. **(F)** MTT assay in 1E4-C9 cells treated or not with 50 nM rapamycin and incubated in serum-free media for 9 days. In **(A,B,E)** Coomassie brilliant blue staining was used as loading control, filled arrowheads show rZNS1-His position whereas hollow arrowheads show the remaining bovine serum albumin contained in the serum-free culture media following a PBS washing step, and the positions of the molecular mass standards are indicated on the left. Data in **(C,D,E,F)** represent mean ± SEM of at least three independent experiments. P-values were calculated by one-way ANOVA, Dunnett's in **(C,D)** and Bonferroni's in **(E,F)**: $^{*}P < 0.05$, $^{**}P < 0.01$, $^{***}P < 0.001$, n.s. not significant.

coworkers reported that rapamycin treatment significantly delayed cell death and enhanced monoclonal antibody production in a hybridoma cell line [49]. To address whether rapamycin could prevent cell death in response to serum depletion in 1E4-C9 cells, we measured cell survival by MTT reduction assay 9 days following 50 nM rapamycin treatment and incubation in serum-free media. We observed that rapamycin treatment did not affect the reduction in cell viability observed for serum starvation (Fig. 2F). As an alternative to rapamycin a pharmacological reagent involved in the regulation of a plethora of cellular pathways such as autophagy induction, we tested whether EBSS a solution with physiological pH that also triggers cellular autophagy [54] had the same effect on rZNS1-His secretion in 1E4-C9 cells. We observed that EBSS led to a similar increase to rapamycin treatment in rZNS1-His secretion at day 9 in serum starved 1E4-C9 cells (Supplementary Fig. 3). Taken together, these results indicate that rZNS1-His protein secretion can be enhanced through at least 50 nM rapamycin or starvation treatment followed by serum-free media incubation for 9 days in 1E4-C9 HEK293 cells.

3.3. Purification of hexameric rZNS1-His protein

In order to purify rZNS1-His, supernatant of 1E4-C9 cells exposed to 50 nM rapamycin and incubated in serum-free media for 9 days was concentrated ~10 times by ultrafiltration using a 100 kDa MWCO disc membrane, dialyzed in 100 mM NaCl - PBS and purified by nickel affinity chromatography. SDS-PAGE analysis showed that rZNS1-His eluted as a single ~48 kDa band in a defined peak, with purity >95 % (Fig. 3A). The average yield of recombinant protein produced in the mammalian expression system described above was ~1 mg of purified rZNS1-His protein per 100 ml of harvested supernatant. The identity of the purified rZNS1-His protein was confirmed by immunoblotting (Fig. 3B). In addition, the analysis showed efficient protein manipulation throughout processing of the supernatant prior to purification. To determine whether rZNS1-His purified from 1E4-C9 cells supernatant presented a hexameric conformation as expected, we carried out a dot blot assay with the harvested supernatant, filtrate (10X concentrated supernatant, >100 kDa) and permeate

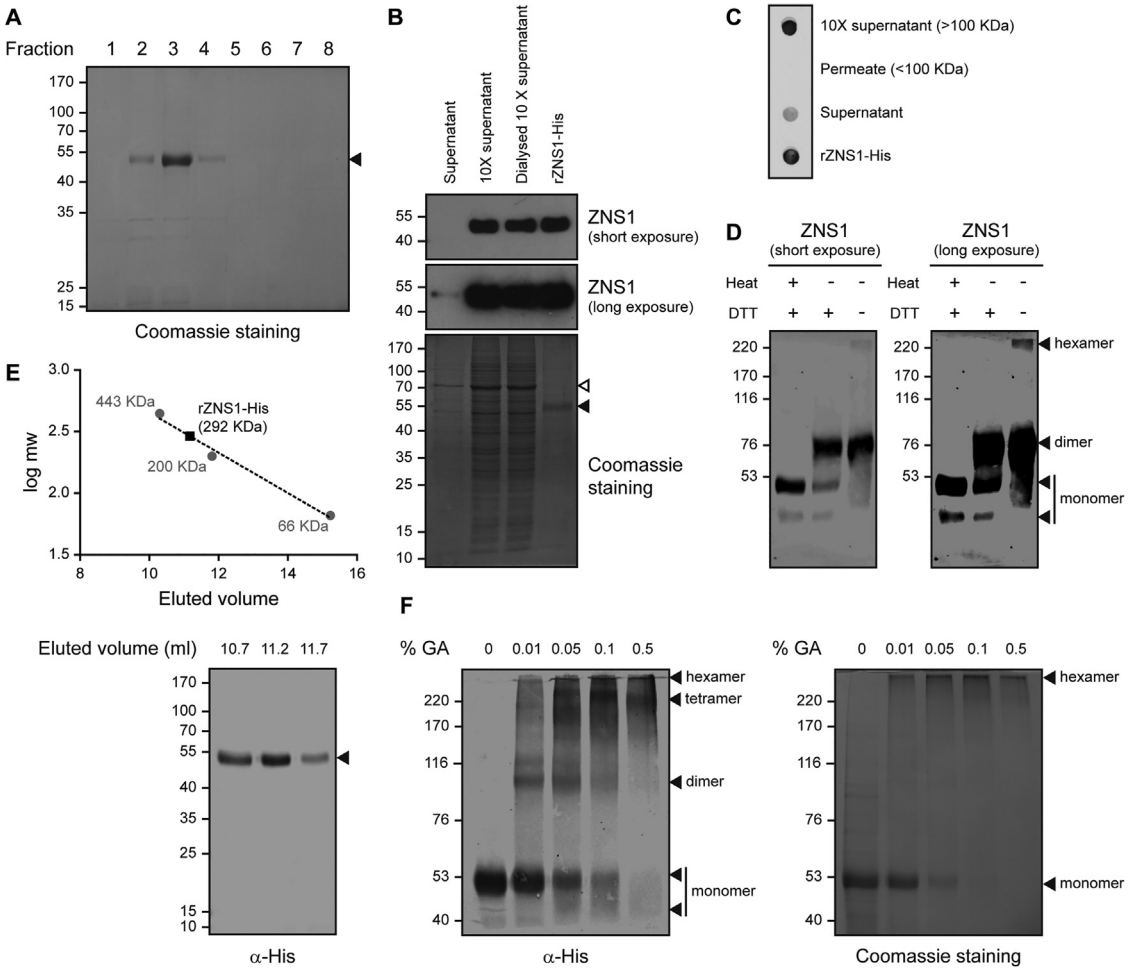

Fig. 3. Purification and conformational characterization of secreted rZNS1-His. **(A)** Nickel affinity chromatography purification of rZNS1-His from 10X dialyzed supernatant of 1E4-C9 cells treated with 50 nM rapamycin and incubated in serum-free media for 9 days. Fractions collected were visualized by Coomassie brilliant blue staining. **(B)** Western blot analysis with anti-ZNS1 monoclonal antibody of 1E4-C9 supernatant processing steps prior to purification by nickel affinity chromatography. Coomassie brilliant blue staining was used as loading control. **(C)** Dot blot analysis with ZNS1 mouse polyclonal sera of 1E4-C9 supernatant, and 10 × 1E4-C9 supernatant or permeate fractions obtained by ultrafiltration with a 100 kDa MWCO disc membrane. **(D)** Immunoblot analysis with anti-ZNS1 monoclonal antibody of purified rZNS1-His subjected or not to heat (5 min 100 °C) and/or 100 mM DTT pretreatment. (**E**) Gel filtration chromatography of rZNS1-His showing a molecular mass corresponding to a hexameric quaternary structure (upper panel), and Western blot analysis with anti-His tag monoclonal antibody of the eluted fractions corresponding to rZNS1-His peak (lower panel). **(F)** In vitro cross-linking of rZNS1-His with different concentrations of glutaraldehyde (GA) analyzed by Western blot with anti-His tag monoclonal antibody (left panel) and with Coomassie brilliant blue staining (right panel). In **(A,B,E)** filled arrowheads show rZNS1-His position whereas in **(B)** hollow arrowheads show the remaining bovine serum albumin contained in the serum-free culture media following a PBS washing step, and in **(A,B,D,E,F)**, the positions of the molecular mass standards are indicated on the left.

(<100 kDa) fractions collected following ultrafiltration, and the purified rZNS1-His protein. No signal was observed in the permeate fraction, suggesting that rZNS1-His protein contained in 1E4-C9 supernatant is a hexamer (Fig. 3C). To further analyze this notion, a SDS-PAGE with purified rZNS1-His under non-denaturing conditions was performed. In the absence of heat denaturation the dimeric conformation was readily detected, while without heat denaturation and under no reducing condition it was possible to visualize the hexameric conformation of rZNS1-His (Fig. 3D). These results are in line with previous reports, which have shown that NS1 dimer is sensitive to heat denaturation [55], and that disulfide bonds contribute to NS1 oligomerization [33]. Finally, we confirmed the quaternary structure of rZNS1-His through gel filtration chromatography, from which we obtained a single peak with a molecular mass of 292 kDa (Fig. 3E), a size compatible with a hexameric conformation. Additionally, we performed a cross-linking assay using different glutaraldehyde concentrations, which resulted in the formation of a predominant complex with a molecular mass compatible with a hexameric form (Fig. 3F). We observed that the absence of heat denaturation (Fig. 3D) generates a faster-migrating dimer species on SDS-PAGE than the dimer detected following glutaraldehyde cross-linking of rZNS1-His (Fig. 3E), which we interpreted as a more compact form of the protein. Collectively, these results indicate that the purified rZNS1-His protein from the supernatant of 1E4-C9 cells is a hexamer as expected.

3.4. rZNS1-His protein is recognized by ZIKV infected patients sera and induces a humoral response in mice

In order to study the potential use of the produced rZNS1-His protein to develop diagnostic tests to detect ZIKV infection, we first characterized the reactivity of anti-NS1 antibodies in ZIKV patient's serum towards rZNS1-His protein. iELISA assays were carried out with the sera of two patients with confirmed ZIKV infection. Data showed that these sera contained IgG antibodies that recognize the purified rZNS1-His protein (Fig. 4A), suggesting that this recombinant protein resembles native NS1 protein conformation and post-translational modifications. Serum from two healthy individuals did not show reactivity to rZNS1-His as expected. Next, we compared the reactivity of ZIKV infected patient's serum against rZNS1-His or the native protein of ZIKV Puerto Rico strain produced to the supernatant of ZIKV infected cells in a dot blot assay. The results revealed that ZIKV patient's serum reacted with rZNS1-His protein as well as with NS1 protein contained in the supernatant of ZIKV infected cells (Fig. 4B). Control serum from a healthy donor did not react towards either of the NS1 proteins. Finally, we sought to establish whether rZNS1-His protein could induce a humoral immune response in a mouse model. To this purpose, mice were immunized intraperitoneally with the recombinant protein and the presence of anti-NS1 antibodies was determined by iELISA after the second booster injection. The results demonstrated the immunogenicity of rZNS1-His protein given that both mice developed an anti-NS1 humoral response (Fig. 4C). Collectively, these results unveil the diagnostic potential of the obtained rZNS1-His protein. Our rZNS1-His protein could potentially be used in the development of anti-NS1 antibody immunocapture assays, as well as in the development of NS1 capture ELISAs and lateral flow systems.

4. Discussion

Zika virus received little attention until 2015 outbreak in Brazil, where a massive epidemic ensued and congenital neurodevelopmental defects were associated with maternal ZIKV infection [2]. Given that ZIKV NS1 hexameric glycoprotein is secreted from the infected cells and released into the patient's bloodstream, typically before or from the onset of the symptoms [56,57], it results in an excellent biomarker for early diagnosis. For these reasons, the present study aimed at establishing a stable and optimized rZNS1 mammalian expression system that would allow the production and purification of the ZNS1 hexamer. Mammalian expression systems are the prevailing method chosen for recombinant protein production among biopharmaceutical companies and academic laboratories. Mammalian cell hosts provide an attractive alternative to prokaryotic hosts since they yield properly folded and assembled proteins, with native-like post-translational modifications [38,58]. In the present work, we developed a rZNS1-His expressing mammalian system through lentiviral transduction followed by dilution cloning of HEK293 cells, which are extensively used for protein over-expression studies [38]. This approach allowed the generation of the 1E4-C9 clone.

Enhancement of protein expression can significantly reduce time and/or cost in the manufacture of many therapeutic proteins. Several reports have shown that an increase in protein production in mammalian cells can be achieved by engineering the host cell, optimizing the culture medium, culturing the cells at low temperature or by the addition of SME to the media [43,59–63]. With this in mind, we tested whether 1E4-C9 secretion of hexameric rZNS1-His could be upregulated by culture medium optimization and SME addition strategies. Serum starvation has been previously used as a medium optimization strategy for increased protein expression purposes [44,45]. We established that the incubation with serum-free media for 9 days yielded the

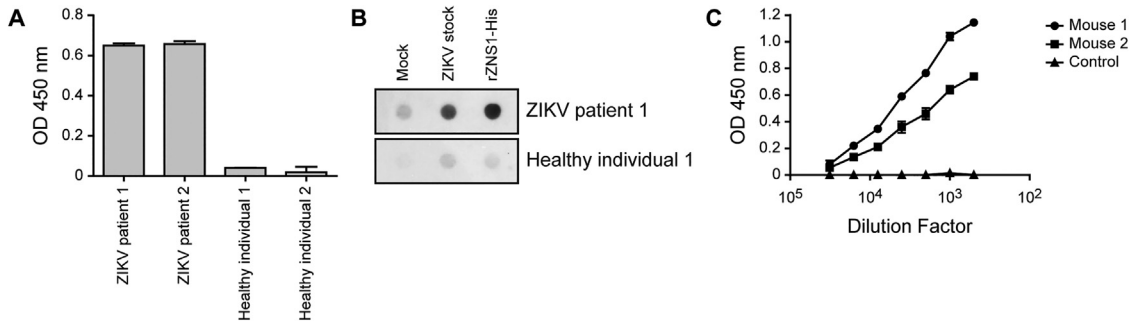

Fig. 4. rZNS1-His reactivity with ZIKV infected patients sera and immunogenicity in a mouse model. **(A)** iELISA of rZNS1-His with serum samples obtained from patients with a positive diagnosis of ZIKV. Healthy individuals sera were used as negative control. Each point of the curve represents mean ± SEM of three sample replicates. **(B)** Dot Blot analysis with the indicated serum samples of rZNS1-His or ZIKV stock obtained from C6/36 cells infected with ZIKV PRVABC59 Puerto Rico strain. Mock-infected C6/36 cells supernatant was loaded as negative control. **(C)** iELISA showing humoral responses of mice immunized with rZNS1-His. Non-immunized mouse sera was used as a negative control. Each point of the curve represents mean ± SD of two sample replicates.

maximum rZNS1-His protein levels. Next, we studied the potential enhancement impact of SME addition to the serum-free media on the already increased rZNS1-His protein levels. The enhancing compound DMSO or hypotonic medium treatment did not affect rZNS1-His secretion. DMSO is an antioxidant that has been reported to increase IL-1β protein production and secretion through transcriptional upregulation [64]. On the other hand, hypotonic medium treatment has been shown to enhance protein expression in a similar mechanism by increasing transcriptional machinery accessibility to the chromatin [51]. Therefore, our results suggest that rZNS1-His production and secretion in 1E4-C9 cells is not affected by a transcriptional pathway boost. Nevertheless, we determined that 50 nM and 100 nM rapamycin treatment followed by incubation for 9 days in serum-free culture medium was able to significantly increase rZNS1-His protein secretion in our mammalian expression system. We presume that this effect occurred in response to rapamycin's ability to reduce the overall cellular biosynthetic burden [65–68], which apparently did not affect our recombinant protein expression. On the other hand, rapamycin is involved in the regulation of a plethora of cellular functions, such as promoting or inhibiting cellular apoptosis [69]. In a previous study, it was reported that rapamycin treatment significantly delayed cell death and enhanced monoclonal antibody production in the CRL 1606 hybridoma cell line [49]. We observed that rapamycin treatment did not prevent serum starvation associated cell death, in line with the notion that the effects of SME rely on the working conditions and the cell lines utilized [43]. Furthermore, rapamycin is a well documented autophagy inducer. Autophagy is a common innate host defense response after viral infection, although it has been reported that this catabolic process can also be utilized by some flavivirus to enhance their replication [70]. In line with this, several studies have indicated that ZIKV induces autophagy by triggering ER stress induction [71–74]. Consistent with these findings, in the current study, rapamycin treatment and subsequent nutrient deprivation through serum-free media incubation, promoted rZNS1-His secretion in 1E4-C9 HEK293 cells. Similar results were obtained by Dupont et. al., who described that IL-1β secretion was upregulated in response to serum deprivation and rapamycin treatment, through an unconventional autophagy-based secretory pathway [75]. As an alternative to rapamycin treatment, we determined that serum starvation following incubation with EBSS a saline solution with physiological pH that is usually used to induce autophagy through starvation pressure, also increased rZNS1-His secretion in 1E4-C9 HEK293 cells. Further experiments should be performed to unravel if rZNS1-His increased secretion following rapamycin and serum-free media incubation is caused by an enhancement of the autophagic flux.

In summary, a stable and optimized rZNS1-His mammalian expression system was developed and characterized. Previous studies have established stable mammalian cell lines that secrete hexameric rZNS1 [76,77]. Viranaicken et al. developed stable rZNS1 Vero cells [77], while Liu et al. established stably transduced HEK293 rZNS1- expressing cells [76]. As Liu's group, we decided to develop a mammalian expression system utilizing HEK293 cell line because it has the advantage of suspension-growing, allowing large-scale culture and protein production. Nevertheless, these studies did not focus on improving the low yield of purified recombinant protein obtained from these expression systems, but rather developed them for research purposes. This is the first work that describes that rapamycin treatment and serum deprivation can upregulate up to 29-fold recombinant ZIKV NS1 protein production in HEK293 cells, reaching protein yields of ∼10 mg/l of culture medium. These conditions may be useful in enhancing research NS1 protein production efficiency and might be considered for large-scale manufacturing of NS1 recombinant protein. The obtained recombinant ZNS1 hexamer is a reliable biological tool of great value for ZIKV clinical diagnosis and surveillance purposes.

CRediT authorship contribution statement

Julieta S. Roldán: Conceptualization, Methodology, Validation, Data curation, Writing - review & editing. **Alejandro Cassola:** Writing - review & editing, Funding acquisition. **Daniela S. Castillo:** Conceptualization, Methodology, Validation, Data curation, Formal analysis, Writing - original draft, Writing - review & editing, Visualization, Supervision.

Declaration of Competing Interest

The authors declare that they have no known competing financial interests or personal relationships that could have appeared to influence the work reported in this paper.

Acknowledgements

We are thankful to Diego Alvarez for his help during lentiviral transduction sessions and for providing ZIKV infected patients sera. The work described in this article was performed with financial support from Agencia Nacional de Promoción Científica y Tecnológica (ANPCyT) [PICT 2016-4813]. AC and DSC are members of the Research Career of CONICET.

Appendix A. Supplementary data

Supplementary material related to this article can be found, in the online version, at doi:https://doi.org/10.1016/j.btre.2020.e00434.

References

[1] G.W. Dick, S.F. Kitchen, A.J. Haddow, Zika virus. I. Isolations and serological specificity, Trans. R. Soc. Trop. Med. Hyg. 46 (1952) 509–520.
[2] A.S. Fauci, D.M. Morens, Zika Virus in the Americas–Yet another arbovirus threat, N. Engl. J. Med. 374 (2016) 601–604.
[3] M.R. Duffy, T.H. Chen, W.T. Hancock, A.M. Powers, J.L. Kool, et al., Zika virus outbreak on Yap Island, Federated States of Micronesia, N. Engl. J. Med. 360 (2009) 2536–2543.
[4] E. Oehler, L. Watrin, P. Larre, I. Leparc-Goffart, S. Lastere, et al., Zika virus infection complicated by Guillain-Barre syndrome–case report, French Polynesia, December 2013, Euro Surveill. 19 (2014).
[5] WHO, WHO Director-General Summarizes the Outcome of the Emergency Committee Regarding Clusters of Microcephaly and Guillain-barré Syndrome, WHO newsletter, 2016.
[6] C.B. Marcondes, F. Ximenes Mde, Zika virus in Brazil and the danger of infestation by Aedes (stegomyia) mosquitoes, Rev. Soc. Bras. Med. Trop. 49 (2016) 4–10.
[7] J.F. Chan, G.K. Choi, C.C. Yip, V.C. Cheng, K.Y. Yuen, Zika fever and congenital Zika syndrome: an unexpected emerging arboviral disease, J. Infect. 72 (2016) 507–524.
[8] G. Venturi, L. Zammarchi, C. Fortuna, M.E. Remoli, E. Benedetti, et al., An autochthonous case of Zika due to possible sexual transmission, Florence, Italy, 2014, Euro Surveill. 21 (2016) 30148.
[9] D.T. Deckard, W.M. Chung, J.T. Brooks, J.C. Smith, S. Woldai, et al., Male-to-Male sexual transmission of zika virus–Texas, January 2016, MMWR Morb. Mortal. Wkly. Rep. 65 (2016) 372–374.
[10] M. Besnard, S. Lastere, A. Teissier, V. Cao-Lormeau, D. Musso, Evidence of perinatal transmission of Zika virus, French Polynesia, December 2013 and February 2014, Euro Surveill. 19 (2014).
[11] J. Lessler, C.T. Ott, A.C. Carcelen, J.M. Konikoff, J. Williamson, et al., Times to key events in Zika virus infection and implications for blood donation: a systematic review, Bull. World Health Organ. 94 (2016) 841–849.
[12] D. Musso, H. Bossin, H.P. Mallet, M. Besnard, J. Broult, et al., Zika virus in French Polynesia 2013-14: anatomy of a completed outbreak, Lancet Infect. Dis. 18 (2018) e172–e182.
[13] V.M. Cao-Lormeau, A. Blake, S. Mons, S. Lastere, C. Roche, et al., Guillain-Barre Syndrome outbreak associated with Zika virus infection in French Polynesia: a case-control study, Lancet 387 (2016) 1531–1539.
[14] P. Brasil, J.P. Pereira Jr, M.E. Moreira, R.M. Ribeiro Nogueira, L. Damasceno, et al., Zika virus infection in pregnant women in Rio De Janeiro, N. Engl. J. Med. 375 (2016) 2321–2334.

[15] C.K. Shapiro-Mendoza, M.E. Rice, R.R. Galang, A.C. Fulton, K. VanMaldeghem, et al., Pregnancy outcomes after maternal zika virus infection during pregnancy - U.S. territories, January 1, 2016-April 25, 2017, MMWR Morb. Mortal. Wkly. Rep. 66 (2017) 615–621.
[16] S. Sukhralia, M. Verma, S. Gopirajan, P.S. Dhanaraj, R. Lal, et al., From dengue to Zika: the wide spread of mosquito-borne arboviruses, Eur. J. Clin. Microbiol. Infect. Dis. 38 (2019) 3–14.
[17] C.M. Rice, *Flaviviridae*: the viruses and their replication, in: B.N. Fields, D. M. K, P.M. Howley (Eds.), Fields Virology, Lippincott-Raven, Philadelphia, Pa, 1996.
[18] G.W. Smith, P.J. Wright, Synthesis of proteins and glycoproteins in dengue type 2 virus-infected vero and Aedes albopictus cells, J. Gen. Virol. 66 (Pt 3) (1985) 559–571.
[19] E.G. Westaway, M.R. Goodman, Variation in distribution of the three flavivirus-specified glycoproteins detected by immunofluorescence in infected Vero cells, Arch. Virol. 94 (1987) 215–228.
[20] G. Winkler, V.B. Randolph, G.R. Cleaves, T.E. Ryan, V. Stollar, Evidence that the mature form of the flavivirus nonstructural protein NS1 is a dimer, Virology 162 (1988) 187–196.
[21] P.W. Mason, Maturation of Japanese encephalitis virus glycoproteins produced by infected mammalian and mosquito cells, Virology 169 (1989) 354–364.
[22] I. Gutsche, F. Coulibaly, J.E. Voss, J. Salmon, J. d'Alayer, et al., Secreted dengue virus nonstructural protein NS1 is an atypical barrel-shaped high-density lipoprotein, Proc. Natl. Acad. Sci. U.S.A. 108 (2011) 8003–8008.
[23] J.M. Mackenzie, M.K. Jones, P.R. Young, Immunolocalization of the dengue virus nonstructural glycoprotein NS1 suggests a role in viral RNA replication, Virology 220 (1996) 232–240.
[24] P. Avirutnan, N. Punyadee, S. Noisakran, C. Komoltri, S. Thiemmeca, et al., Vascular leakage in severe dengue virus infections: a potential role for the nonstructural viral protein NS1 and complement, J. Infect. Dis. 193 (2006) 1078–1088.
[25] D.S. Sun, C.C. King, H.S. Huang, Y.L. Shih, C.C. Lee, et al., Antiplatelet autoantibodies elicited by dengue virus non-structural protein 1 cause thrombocytopenia and mortality in mice, J. Thromb. Haemost. 5 (2007) 2291–2299.
[26] J.H. Huang, J.J. Wey, Y.C. Sun, C. Chin, L.J. Chien, et al., Antibody responses to an immunodominant nonstructural 1 synthetic peptide in patients with dengue fever and dengue hemorrhagic fever, J. Med. Virol. 57 (1999) 1–8.
[27] P.Y. Shu, L.K. Chen, S.F. Chang, Y.Y. Yueh, L. Chow, et al., Comparison of capture immunoglobulin M (IgM) and IgG enzyme-linked immunosorbent assay (ELISA) and nonstructural protein NS1 serotype-specific IgG ELISA for differentiation of primary and secondary dengue virus infections, Clin. Diagn. Lab. Immunol. 10 (2003) 622–630.
[28] P.Y. Shu, L.K. Chen, S.F. Chang, C.L. Su, L.J. Chien, et al., Dengue virus serotyping based on envelope and membrane and nonstructural protein NS1 serotype-specific capture immunoglobulin M enzyme-linked immunosorbent assays, J. Clin. Microbiol. 42 (2004) 2489–2494.
[29] D.A. Muller, P.R. Young, The flavivirus NS1 protein: molecular and structural biology, immunology, role in pathogenesis and application as a diagnostic biomarker, Antiviral Res. 98 (2013) 192–208.
[30] J. Lessler, L.H. Chaisson, L.M. Kucirka, Q. Bi, K. Grantz, et al., Assessing the global threat from Zika virus, Science 353 (2016) aaf8160.
[31] B.J. Blitvich, D. Scanlon, B.J. Shiell, J.S. Mackenzie, K. Pham, et al., Determination of the intramolecular disulfide bond arrangement and biochemical identification of the glycosylation sites of the nonstructural protein NS1 of Murray Valley encephalitis virus, J. Gen. Virol. 82 (2001) 2251–2256.
[32] T.P. Wallis, C.Y. Huang, S.B. Nimkar, P.R. Young, J.J. Gorman, Determination of the disulfide bond arrangement of dengue virus NS1 protein, J. Biol. Chem. 279 (2004) 20729–20741.
[33] M.J. Pryor, P.J. Wright, The effects of site-directed mutagenesis on the dimerization and secretion of the NS1 protein specified by dengue virus, Virology 194 (1993) 769–780.
[34] M.J. Pryor, P.J. Wright, Glycosylation mutants of dengue virus NS1 protein, J. Gen. Virol. 75 (Pt 5) (1994) 1183–1187.
[35] G. Winkler, S.E. Maxwell, C. Ruemmler, V. Stollar, Newly synthesized dengue-2 virus nonstructural protein NS1 is a soluble protein but becomes partially hydrophobic and membrane-associated after dimerization, Virology 171 (1989) 302–305.
[36] A.J. Crooks, J.M. Lee, L.M. Easterbrook, A.V. Timofeev, J.R. Stephenson, The NS1 protein of tick-borne encephalitis virus forms multimeric species upon secretion from the host cell, J. Gen. Virol. 75 (Pt 12) (1994) 3453–3460.
[37] M. Flamand, F. Megret, M. Mathieu, J. Lepault, F.A. Rey, et al., Dengue virus type 1 nonstructural glycoprotein NS1 is secreted from mammalian cells as a soluble hexamer in a glycosylation-dependent fashion, J. Virol. 73 (1999) 6104–6110.
[38] A.C. Dalton, W.A. Barton, Over-expression of secreted proteins from mammalian cell lines, Protein Sci. 23 (2014) 517–525.
[39] C.R. Parrish, W.S. Woo, P.J. Wright, Expression of the NS1 gene of dengue virus type 2 using vaccinia virus. Dimerisation of the NS1 glycoprotein, Arch. Virol. 117 (1991) 279–286.
[40] H. Leblois, P.R. Young, Maturation of the dengue-2 virus NS1 protein in insect cells: effects of downstream NS2A sequences on baculovirus-expressed gene constructs, J. Gen. Virol. 76 (Pt 4) (1995) 979–984.
[41] D.S. Castillo, A. Campalans, L.M. Belluscio, A.L. Carcagno, J.P. Radicella, et al., E2F1 and E2F2 induction in response to DNA damage preserves genomic stability in neuronal cells, Cell Cycle 14 (2015) 1300–1314.
[42] J.A. Muller, M. Harms, A. Schubert, S. Jansen, D. Michel, et al., Inactivation and environmental stability of zika virus, Emerging Infect. Dis. 22 (2016) 1685–1687.
[43] M.J. Allen, J.P. Boyce, M.T. Trentalange, D.L. Treiber, B. Rasmussen, et al., Identification of novel small molecule enhancers of protein production by cultured mammalian cells, Biotechnol. Bioeng. 100 (2008) 1193–1204.
[44] S. Dong, A. Khoo, J. Wei, R.K. Bowser, N.M. Weathington, et al., Serum starvation regulates E-cadherin upregulation via activation of c-Src in non-small-cell lung cancer A549 cells, Am. J. Physiol., Cell Physiol. 307 (2014) C893–899.
[45] M.U. Rashid, K.M. Coombs, Serum-reduced media impacts on cell viability and protein expression in human lung epithelial cells, J. Cell. Physiol. 234 (2019) 7718–7724.
[46] F. Braun, J. Bertin-Ciftci, A.S. Gallouet, J. Millour, P. Juin, Serum-nutrient starvation induces cell death mediated by Bax and Puma that is counteracted by p21 and unmasked by Bcl-x(L) inhibition, PLoS One 6 (2011) e23577.
[47] A.A. Goyeneche, J.M. Harmon, C.M. Telleria, Cell death induced by serum deprivation in luteal cells involves the intrinsic pathway of apoptosis, Reproduction 131 (2006) 103–111.
[48] C.H. Liu, L.H. Chen, Promotion of recombinant macrophage colony stimulating factor production by dimethyl sulfoxide addition in Chinese hamster ovary cells, J. Biosci. Bioeng. 103 (2007) 45–49.
[49] R.R. Balcarcel, G. Stephanopoulos, Rapamycin reduces hybridoma cell death and enhances monoclonal antibody production, Biotechnol. Bioeng. 76 (2001) 1–10.
[50] A.K. Shukla, C. Reinhart, H. Michel, Dimethylsulphoxide as a tool to increase functional expression of heterologously produced GPCRs in mammalian cells, FEBS Lett. 580 (2006) 4261–4265.
[51] M.F. Ogara, P.F. Sirkin, A.L. Carcagno, M.C. Marazita, S.V. Sonzogni, et al., Chromatin relaxation-mediated induction of p19INK4d increases the ability of cells to repair damaged DNA, PLoS One 8 (2013) e61143.
[52] M. Downey, D. Durocher, Chromatin and DNA repair: the benefits of relaxation, Nat. Cell Biol. 8 (2006) 9–10.
[53] D.V. Oliveira, A. Kato, K. Nakamura, T. Ikura, M. Okada, et al., Histone chaperone FACT regulates homologous recombination by chromatin remodeling through interaction with RNF20, J. Cell. Sci. 127 (2014) 763–772.
[54] C. Liu, E.P. DeRoo, C. Stecyk, M. Wolsey, M. Szuchnicki, et al., Impaired autophagy in mouse embryonic fibroblasts null for Kruppel-like Factor 4 promotes DNA damage and increases apoptosis upon serum starvation, Mol. Cancer 14 (2015) 101.
[55] S. Noisakran, T. Dechtawewat, P. Rinkaewkan, C. Puttikhunt, A. Kanjanahaluethai, et al., Characterization of dengue virus NS1 stably expressed in 293T cell lines, J. Virol. Methods 142 (2007) 67–80.
[56] S. Alcon, A. Talarmin, M. Debruyne, A. Falconar, V. Deubel, et al., Enzyme-linked immunosorbent assay specific to Dengue virus type 1 nonstructural protein NS1 reveals circulation of the antigen in the blood during the acute phase of disease in patients experiencing primary or secondary infections, J. Clin. Microbiol. 40 (2002) 376–381.
[57] L. Thomas, F. Najioullah, O. Verlaeten, J. Martial, S. Brichler, et al., Relationship between nonstructural protein 1 detection and plasma virus load in Dengue patients, Am. J. Trop. Med. Hyg. 83 (2010) 696–699.
[58] J. Zhu, Mammalian cell protein expression for biopharmaceutical production, Biotechnol. Adv. 30 (2012) 1158–1170.
[59] K. Chen, Q. Liu, L. Xie, P.A. Sharp, D.I. Wang, Engineering of a mammalian cell line for reduction of lactate formation and high monoclonal antibody production, Biotechnol. Bioeng. 72 (2001) 55–61.
[60] G. Seth, P. Hossler, J.C. Yee, W.S. Hu, Engineering cells for cell culture bioprocessing–physiological fundamentals, Adv. Biochem. Eng. Biotechnol. 101 (2006) 119–164.
[61] C. Altamirano, C. Paredes, A. Illanes, J.J. Cairo, F. Godia, Strategies for fed-batch cultivation of t-PA producing CHO cells: substitution of glucose and glutamine and rational design of culture medium, J. Biotechnol. 110 (2004) 171–179.
[62] L. Xie, D.I. Wang, High cell density and high monoclonal antibody production through medium design and rational control in a bioreactor, Biotechnol. Bioeng. 51 (1996) 725–729.
[63] J. Rodriguez, M. Spearman, N. Huzel, M. Butler, Enhanced production of monomeric interferon-beta by CHO cells through the control of culture conditions, Biotechnol. Prog. 21 (2005) 22–30.
[64] L. Xing, D.G. Remick, Mechanisms of dimethyl sulfoxide augmentation of IL-1 beta production, J. Immunol. 174 (2005) 6195–6202.
[65] P.B. Mahajan, Modulation of transcription of rRNA genes by rapamycin, Int. J. Immunopharmacol. 16 (1994) 711–721.
[66] R.J. White, Regulation of RNA polymerases I and III by the retinoblastoma protein: a mechanism for growth control? Trends Biochem. Sci. 22 (1997) 77–80.
[67] D. Zaragoza, A. Ghavidel, J. Heitman, M.C. Schultz, Rapamycin induces the G0 program of transcriptional repression in yeast by interfering with the TOR signaling pathway, Mol. Cell. Biol. 18 (1998) 4463–4470.
[68] H. Kawasome, P. Papst, S. Webb, G.M. Keller, G.L. Johnson, et al., Targeted disruption of p70(s6k) defines its role in protein synthesis and rapamycin sensitivity, Proc. Natl. Acad. Sci. U.S.A. 95 (1998) 5033–5038.
[69] M. Castedo, K.F. Ferri, G. Kroemer, Mammalian target of rapamycin (mTOR): pro- and anti-apoptotic, Cell Death Differ. 9 (2002) 99–100.
[70] L.A. Carneiro, L.H. Travassos, Autophagy and viral diseases transmitted by Aedes aegypti and Aedes albopictus, Microbes Infect. 18 (2016) 169–171.

[71] Q. Liang, Z. Luo, J. Zeng, W. Chen, S.S. Foo, et al., Zika virus NS4A and NS4B proteins deregulate Akt-mTOR signaling in human fetal neural stem cells to inhibit neurogenesis and induce autophagy, Cell Stem Cell 19 (2016) 663–671.
[72] H. Peng, B. Liu, T.D. Yves, Y. He, S. Wang, et al., Zika virus induces autophagy in human umbilical vein endothelial cells, Viruses 10 (2018).
[73] A.I. Chiramel, S.M. Best, Role of autophagy in Zika virus infection and pathogenesis, Virus Res. 254 (2018) 34–40.
[74] R. Gratton, A. Agrelli, P.M. Tricarico, L. Brandao, S. Crovella, Autophagy in Zika Virus Infection: A Possible Therapeutic Target to Counteract Viral Replication, Int. J. Mol. Sci. 20 (2019).
[75] N. Dupont, S. Jiang, M. Pilli, W. Ornatowski, D. Bhattacharya, et al., Autophagy-based unconventional secretory pathway for extracellular delivery of IL-1beta, EMBO J. 30 (2011) 4701–4711.
[76] J. Liu, P. Wan, Q. Li, X. Li, A. Li, et al., Construction and identification of recombinant HEK293T cell lines expressing non-structural protein 1 of zika virus, Int. J. Med. Sci. 14 (2017) 1072–1079.
[77] W. Viranaicken, A. Ndebo, S. Bos, P. Souque, G. Gadea, et al., Recombinant zika NS1 protein secreted from vero cells is efficient for inducing production of immune serum directed against NS1 dimer, Int. J. Mol. Sci. 19 (2017).